04

Conducting fundamental scientific research and exploratory scientific research

© D.N. Mirkhanov, Al.F. Gaisin, R.Sh. Basyrov, S.Yu. Petryakov

Tupolev Kazan National Research Technical University (KAI),
Kazan, Tatarstan, Russia
e-mail: almaz87@mail.ru

Received December 7, 2022
Revised January 19, 2023
Accepted January 22, 2023

The work is devoted to the study of the characteristics of a low-temperature plasma of a high-frequency (HF) discharge ($f = 13.56$ MHz) ignited between metallic and electrolytic electrodes at atmospheric pressure. Burning of an RF discharge in a diffuse (volumetric) form is observed at the interface between the media between the electrodes. Numerical calculations of the electric field strength and the distribution of the volumetric power density of the Joule heat release before breakdown in a vapor-gas mixture near a metal electrode are presented. The discharge radiation spectrum, plasma composition, and electron density were studied by optical emission spectroscopy. The thermograms of the electrode surface under the conditions of an RF discharge are considered.

Keywords: Plasma-liquid systems, high-frequency discharge, electrolytes, numerical methods.

DOI: 10.21883/TP.2023.03.55806.267-22

Introduction

Low-temperature plasma of discharges with liquid (non-metallic) electrodes is a rapidly developing interdisciplinary field of studies, including the science of plasma, heat and mass transfer, fluid and gas dynamics, photolysis, and multiphase chemistry [1]. Discharges in plasma-liquid systems are generated by direct or alternating current in the interelectrode space, where fluid is used as one of the electrodes. As a rule, as liquid electrode the solutions of salts of various concentrations in distilled, technical or purified tap water are used. The discharge is ignited in gas-discharge chambers with various types and configurations of electrodes, including systems: solid−liquid electrodes [2–5], liquid (flow)−liquid (non-flow) electrodes [6], liquid (flow)−liquid (flow) electrodes [7]. The most common discharge ignition schemes are implemented when a metal electrode is immersed in an electrolyte [8], or when the metal electrode is located at some distance from the electrolyte surface [9]. The ambient air pressure used in the studies is limited to the range of 10^5-10^3 Pa, since at lower pressures the solution begins to boil in the electrolytic cells of the gas discharge chamber.

Discharges with liquid (non-metallic) electrodes are of great interest for solving various applied problems in the field of mechanical engineering, metalwork, and medicine. Specialists from various scientific schools are studying the use of discharges with liquid electrodes for treatment of products with complex geometry of the outer and inner surfaces, made both using traditional production methods (stamping, casting, etc.) [10–12], and additive methods of laser sintering of metal powders [13]. The results of the plasma-liquid systems use for the production of finely dispersed metal powders and the production of nanoparticles, the application of functional coatings on products, the analysis of particles content in liquids, plasma-chemical reactors, sterilization and purification of solids, water and air are presented in foreign and domestic publications [14]. A wide variety of these systems application is due to a large number of configurations of gas discharge chambers, modes and parameters of discharge ignition and combustion, as well as common plasma-chemical processes associated with the transfer of matter and charge at the interface.

An analysis of published works shows that the most studied in the field of plasma-liquid systems are direct current discharges, some of which are formed as technologies and implemented at mechanical engineering and metalworking enterprises, where they are successfully used to treat the surface of metal products in order to improve their performances.

At the same time, the number of „white spots“ in this field of science is still large. For example, high-frequency discharges with liquid (non-metallic) electrodes are still little studied, while the scientific foundations of high-frequency discharges between solid electrodes are described in detail in the well-known papers of Yu.P. Raiser, M.N. Schneider, N.A. Yatsenko and others [15].

Discharges with liquid (non-metallic) electrodes mix in a complex way three subsystems describing, respectively, the physics of processes in the plasma (HF discharge), liquid (non-flowing and flowing electrolyte), and gas (ambient air) phase states. In these systems there are more than 50 charged, neutral atomic and molecular particles, which enter into more than 600 reactions with each other and affect the energy balance in the discharge [16]. This is the reason for the complexity of the numerical works. The results obtained

in this case do not correlate well with the experimental data. All this makes it difficult to create a unified classification of plasma-liquid systems, similar to classification that exists for discharges with solid electrodes (spark, arc, glow, corona, etc.) [17].

One of the possible directions of systematization of discharges with liquid electrodes is their classification by elementary processes, therefore, carrying out search work and numerical calculations, which are qualitatively and quantitatively consistent with experimental data, are an urgent task. The authors earlier published the results of studies of RF discharges in systems where both electrodes are liquid, including those with jet electrodes [18,19]. The electrophysical, thermal and spectral parameters of the discharge were studies. On the basis of the conducted experimental studies the numerical calculations were carried out, as a result of which the physical mechanism for the occurrence of ring and semi-ring plasma structures around an electrolyte jet in RF discharge was described. It is shown that the electric field strength in the jet flow decay region can reach the values 10^9-10^{10} V/m, at which autoelectronic emission is possible, leading to the appearance of primary electrons in the vicinity of the jet, which leads to ionization and excitation of the molecules of the surrounding gaseous medium.

The purpose of this work is to study the properties of RF discharge when metal electrode is immersed in the electrolyte at atmospheric pressure. To interpret the breakdown conditions in the gas-vapor mixture near metal electrode, the numerical calculations of the electric field strength and the distribution of the volumetric power density of the Joule heat release were carried out. The results obtained can be used to develop mathematical models of plasma-liquid systems of RF discharge in the electrode configuration under consideration, as well as to create plasma devices.

1. Experimental setup

Ignition and study of the RF discharge were carried out on the experimental setup with a gas-discharge chamber (Fig. 1) at set parameters of voltage $U = 0.1-4$ kV, pressure $p = 10^5$ Pa, the diameter of the metal rod $d_t = 4-7$ mm, the depth of the metal rod immersion in the electrolyte $h = 0-3$ mm, the interelectrode gap $i = 1-5$ mm (distance between the metal electrode and the electrolyte when it rises above the surface of the solution). The experimental setup is equipped with HF generator „VChG8-60/13“ with operating frequency of 13.56 MHz and oscillatory power of 60 kW. The generator is designed to heat dielectric materials and to power technological devices. A metal rod made by selective laser sintering from fine powder „StainlessSteel PH1“ on Electro Optical Systems (EOS) 3*D* printer was used as a metal electrode. Approximate chemical composition of the powder: iron — 75%, chromium — 15%, nickel — 4.5%, copper — 3.5%). The electrolyte was 3% NaCl

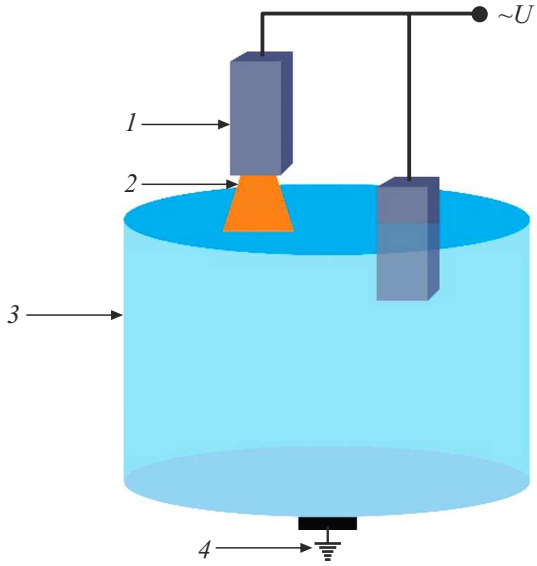

Figure 1. Functional diagram of the work chamber for maintaining RF discharge between metallic and liquid (non-metallic) electrodes: *1* — loaded electrode, *2* — RF discharge, *3* — bath with electrolyte, *4* — grounding of setup casing.

solution in purified tap water. The metal rod, which was a loaded electrode, was immersed in the grounded cell with electrolyte and moved in vertical plane at a distance of 8 mm using automatic manipulator. A thermostat is provided to control the electrolyte solution temperature in the bath. Thermostating of the electrolyte was carried out using a circulation cooler of a refrigerator type. The renewal of the electrolyte in the bath was carried out using the electrolyte supply and removal system. To clean the solution from impurities, a coarse filter is provided in the system. The electrolyte vapors were removed from the discharge study zone using a stationary exhaust and fan.

To solve the tasks set in the paper, modern methods and research approaches were used.

1. Video shooting of the dynamics of the processes occurring in the combustion zone of RF discharge between the metallic and electrolytic electrodes, as well as the plasma structures formed in this case, was carried out using a high-speed video camera „Casio EX-F1“. In view of the high dynamicity of the processes occurring in the combustion zone of the discharge, the shooting speed was chosen to be 1200 and 600 fps. The camera was mounted on a tripod at a distance of 300 mm from the discharge burning zone, which transmitted the received information to computer with an operator. The received data were processed on personal computer with installed software „HX Link“ and „Movavi Video Editor 14 Plus“. An additional detailed study of plasma structures on the surface of liquid and metallic electrodes was carried out simultaneously using „SP-52“ microscope.

2. The RF discharge plasma radiation was analyzed by emission spectroscopy on a „PLASUS EC 150201 MC“

optical fiber spectrometer. The discharge radiation was registered using a collimator for registration light rays in the wavelength range 195−1105 nm. The collimator was brought to the discharge burning zone at a distance of 100−200 mm. The instrumental function of the system was calibrated by recording light radiation from the lamp „SIRSh 6-100". The width of the minimum, single and narrowest lines of the spectrum was taken as the instrumental width, which turned out to be equal to $\Delta\lambda_g = 1$ nm. The studied radiation was collected from the entire volume of the formed discharge; therefore, the composition and components of the plasma were estimated without reference to a specific point on the discharge. The data obtained were analyzed by comparing the studied spectrum with the database of the National Institute of Standards and Technology (NIST, USA).

3. To analyze the temperature distribution of the studied surface of the metallic and electrolytic electrodes during the combustion of the RF discharge, a „FLIRA6500SC" thermal imaging camera with a detector spatial resolution of 640 × 512 pixels was used with an operating spectral range of 3.6−4.9 μm. The thermal imager provided reading of the electrode surface temperature in the calibrated range 4−2400°C. The obtained values were processed on computer with „ALTAIR v5.91.010" software.

4. Studies of fluctuations of current and voltage of HF discharge were carried out with a „AKTAKOM ASK-2067" digital oscilloscope with a high-frequency voltage divider „Elektronika R6015A".

5. Numerical calculations were carried out in the „MATLAB" environment. The flow of HF current in the electrolytic cell with grounded conductive bottom was considered. The problem was solved using the finite element method, the computational domain was divided into elements in the form of tetrahedra. The model includes Maxwell's equations for the electric and magnetic field strengths, the current density vector, and the electric field potential.

2. Results and discussion

Ignition of HF discharge by the contact method using metallic electrode with diameter of 4 mm with electrolyte surface showed that when the voltage is set to 1 kV, the process of evaporation is initialized in the region of interaction of the electrodes, and then the boiling of the electrolyte starts with intense vaporization, which occurs both on the free surface of the liquid, and around the metallic electrode. In this case, interface appears around the metal electrode, i.e., bubbles form on its surface, which contain air and saturated steam. The RF current in the circuit drives the processes of chemical separation of dissolved substances from the electrolyte and Joule heat release from the surface of the metallic electrode. A process characteristic for electrolysis takes place in the gas-discharge chamber. By changing the parameters of temperature and concentration of the electrolyte, it is possible to change near-electrode processes in the desired direction. Breakdown at the interface does not occur, since the power supplied to the RF discharge is not sufficient to ionize the vapor-air mixture and cause an electron avalanche.

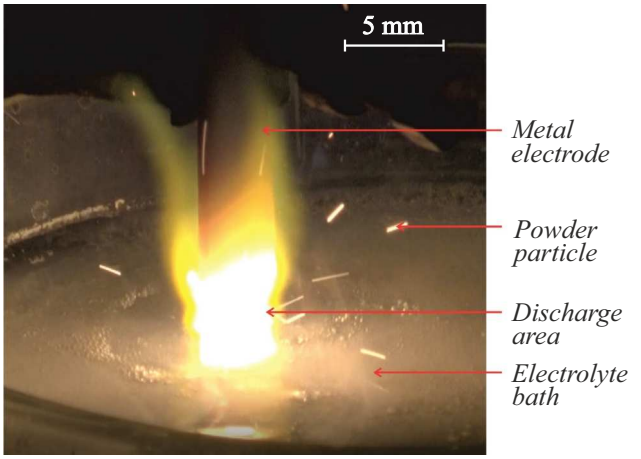

Figure 2. Photo of RF discharge burning between metallic and liquid (non-metallic) electrodes.

In the voltage range from 1 to 3 kV the electric field strength reaches values sufficient to initiate the electron avalanche during the breakdown of the gas-vapor gap. After the breakdown of the gas-vapor gap, the formation of free electrons in HF discharge can be affected by ionization by direct electron impact, step, photo- and dissociative ionization in the volume, as well as plasma-chemical reactions between dissociation products at the electrolyte boundary and in the volume. After the breakdown the metallic electrode from the immersed state was raised above the electrolyte surface with the help of hydraulic drive. From the analysis of high-speed shooting it was found that the HF discharge is formed in the form of microchannels that pulsate in the vapor-air mixture around the metallic electrode. With increase in voltage over 3.5 kV, the RF discharge passes into the volumetric (diffuse) combustion mode (Fig. 2).

The analysis of the oscillograms showed that the fluctuations in the current and voltage of RF discharge have non-sinusoidal and asymmetric form. Along with this, HF pulsations are observed at the fundamental harmonic of oscillations ($f = 13.56$ MHz). The range of oscillations of RF discharge current varies from 10 to 18 A. The combustion of volumetric (diffuse) HF discharge is accompanied by an intense release of convective vapor-air flows, the formation of drops, by acoustic pops, and the spraying of the metallic electrode over the liquid surface with the deposition of a finely dispersed metal powder at the bottom of the electrolytic cell. The change in the dynamics of the processes occurring at the interface is explained by increase in the power supplied to the RF discharge. Due to the gradual destruction of the metallic electrode surface

by the discharge, the interelectrode distance increases, and the discharge goes out. An automatic manipulator was used to maintain the optimal interelectrode distance in order to stabilize the RF discharge.

To interpret the breakdown conditions in the vapor-gas mixture near the metallic electrode, numerical calculations of the electric field strength and the distribution of the volume density of the Joule heat release power were carried out. The flow of high-frequency current in electrolytic cell with grounded conductive bottom is considered (Fig. 1). The metallic cylindrical electrode is partially immersed in the electrolyte, and voltage is applied to it from high-frequency voltage source with frequency of $f = 13.56$ MHz. Electrolyte — 3% NaCl solution in technical water.

The of Maxwell system equations was used for the calculation in the absence of free charges

$$\mathrm{rot}\mathbf{E} = -\mu_0\mu \frac{\partial \mathbf{H}}{\partial t}, \tag{1}$$

$$\mathrm{rot}\mathbf{H} = \varepsilon_0\varepsilon \frac{\partial \mathbf{E}}{\partial t} + \mathbf{j}, \tag{2}$$

where is the conduction current density vector is

$$\mathbf{j} = \sigma\mathbf{E}. \tag{3}$$

Applying the rotor operator to both sides of equation (1) and using (2), we eliminate the magnetic field strength

$$\mathrm{rot}\,\mathrm{rot}\mathbf{E} = -\varepsilon_0\varepsilon\mu_0\mu \frac{\partial^2 \mathbf{E}}{\partial t^2} - \mu_0\mu \frac{\partial \mathbf{j}}{\partial t}. \tag{4}$$

There is an identity

$$\mathrm{rot}\,\mathrm{rot}\mathbf{E} = \mathrm{grad}\,\mathrm{div}\mathbf{E} - \Delta\mathbf{E}.$$

In the absence of space charges

$$\mathrm{div}\mathbf{E} = 0,$$

then

$$-\Delta\mathbf{E} + \varepsilon_0\varepsilon\mu_0\mu \frac{\partial^2 \mathbf{E}}{\partial t^2} + \mu_0\mu\sigma \frac{\partial \mathbf{E}}{\partial t} = 0. \tag{5}$$

A harmonically changing field can be represented in a complex form

$$\mathbf{E} = \mathbf{E}_c e^{j\omega t}, \tag{6}$$

where $\mathbf{E}_c$ — complex amplitude, $\omega = 2\pi f$ — cyclic frequency, j — imaginary unit.

Substituting (6) into (5), we obtain the equation for the complex amplitude of the electric field strength

$$-\Delta\mathbf{E}_c + \varepsilon_0\mu_0\mu\omega^2\left(j\frac{\sigma}{\omega\varepsilon_0} - \varepsilon\right)\mathbf{E}_c = 0. \tag{7}$$

Relative permittivity ε and conductivity σ of electrolyte depend on temperature, solution concentration and electromagnetic field frequency.

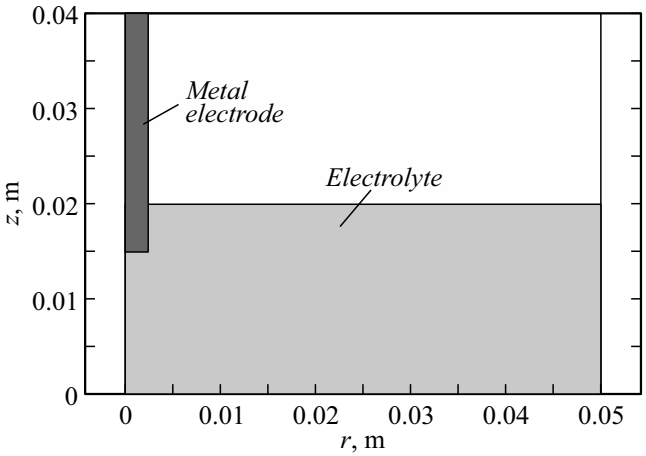

Figure 3. Geometry of computational domain: z — vertical coordinate, r — radial coordinate.

Empirical models for calculating these parameters for NaCl solution (model M22, [20]) are presented. The value of static permittivity calculated by this model for 3% NaCl solution (salinity $S = 30\%$) is $\varepsilon_S = 78$, ionic conductivity $\sigma = 4.87$ S/m.

In expression (7), the multiplier $\sigma/(\omega\varepsilon_0)$ characterizes the scattering caused by the conduction current, and ε — the scattering caused by the bias current. The transition frequency of electromagnetic wave f_t is defined as the frequency at which the conduction current is equal to the bias current: $\sigma/(2\pi f_t\varepsilon_0) = \varepsilon$, hence $f_t = \sigma/(2\pi\varepsilon_0\varepsilon)$. The conduction current is greater than the bias current at frequencies $f < f_t$ and less than the bias current at frequencies $f > f_t$. The value of the transition frequency calculated from the static values of the conductivity and permittivity for the NaCl solution is $f_t \approx 2.5$ GHz.

In the considered case of the HF field frequency $f = 13.56$ MHz we have $f \ll f_t$, so the static values for ε and σ can be applied in the calculations.

Assuming the presence of axial symmetry around the electrode axis, we will consider the problem in cylindrical coordinates (r, z) (Fig. 3). Let the amplitude of the HF voltage applied to the electrode be U_m. Using the homogeneity of equation (7) instead of the vector $\mathbf{E}_c$ the problem can be solved with respect to the value $\tilde{\mathbf{E}}_c = \mathbf{E}_c/U_m$ — reduced strength (measured in 1/m).

The equations for the radial $\tilde{E}_r$ and vertical $\tilde{E}_z$ components of the electric field strength in a cylindrical coordinate system have the form

$$-\frac{1}{r}\frac{\partial}{\partial r}\left(r\frac{\partial \tilde{E}_r}{\partial r}\right) - \frac{\partial^2 \tilde{E}_r}{\partial z^2} + \frac{\tilde{E}_r}{r^2} + \mu\frac{\omega^2}{c^2}\left(j\frac{\sigma}{\omega\varepsilon_0} - \varepsilon\right)\tilde{E}_r = 0, \tag{8}$$

$$-\frac{1}{r}\frac{\partial}{\partial r}\left(r\frac{\partial \tilde{E}_z}{\partial r}\right) - \frac{\partial^2 \tilde{E}_z}{\partial z^2} + \mu\frac{\omega^2}{c^2}\left(j\frac{\sigma}{\omega\varepsilon_0} - \varepsilon\right)\tilde{E}_z = 0. \tag{9}$$

Here the relation $\varepsilon_0\mu_0 = 1/c^2$ is taken into account.

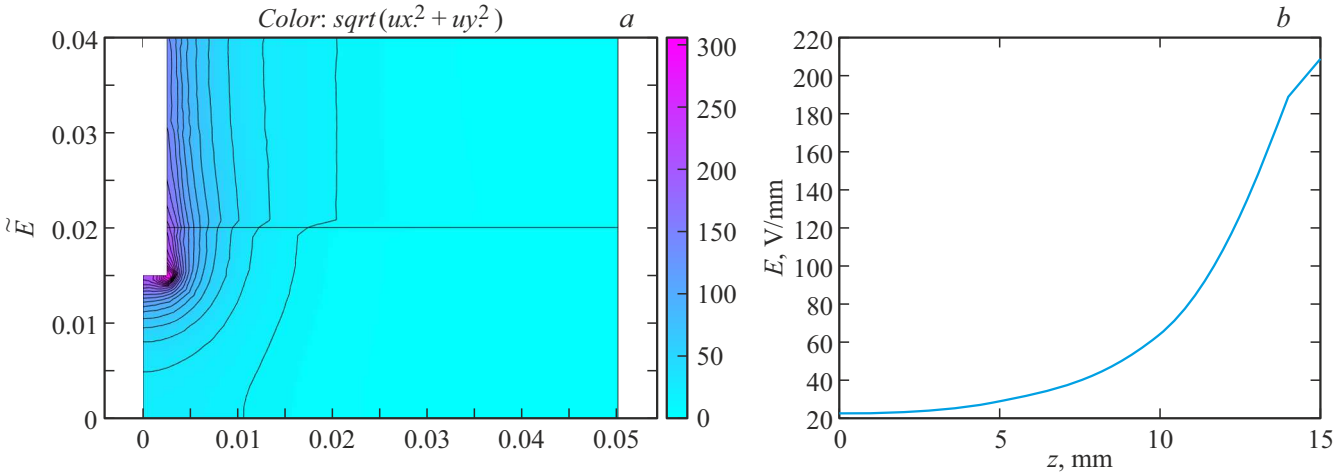

Figure 4. Isolines of modulus of strength vector $\tilde{E}$ (a) and the electric field strength E on the symmetry axis $(r = 0)$ in the interval from the bottom plate to the electrode (b).

To solve equations $(8), (9)$ it is necessary to set boundary conditions. On conducting surfaces, the tangent component of the field strength vector turns to 0: $\tilde{E}_r(r, 0) = 0$ on the lower grounded plate; $\tilde{E}_z(R, 0) = 0$ on the electrode surface, R — electrode radius $(R = 0.0025\,\text{m})$; on the symmetry axis $\tilde{E}_r(0, z) = 0$.

To set the normal components of the field strength vector on conducting surfaces, one can use the fact that at frequencies $f \ll f_t$ the field can be considered slowly changing, and the equation for the scalar potential of the electric field can be solved

$$\text{div}\mathbf{j} = \text{div}\sigma\mathbf{E} = 0,$$

$$\mathbf{E} = -\text{grad}\varphi,$$

$$\text{div}(\sigma\,\text{grad}\varphi) = 0. \qquad (10)$$

For equation (10), the value of the potential on the electrode $\varphi = U_m$, on the grounded plate $\varphi = 0$ is set.

Equation (10), and then equations $(8), (9)$ were solved in the MATLAB by the equations solver in partial differentials pdetool.

Fig. 4, a shows lines of constant value of the strength modulus $\tilde{E} = \sqrt{\tilde{E}_r^2 + \tilde{E}_z^e}$. Fig. 4, b shows the field strength modulus versus z in the gap between the electrode and the bottom plate at $U_m = 1000\,\text{V}$. It can be seen from the graph that near the metallic electrode E reaches 210 V/mm. This is due to the strong heterogeneity of the electric field near the rod metallic electrode. In the zero potential direction E falls non-linearly.

The distribution of the volumetric power density of the Joule heat release $\tilde{w} = \sigma\tilde{E}^2$ near the electrode is shown in Fig. 5, a. The greatest heat release occurs near the edge of the electrode, where the electric field is highly heterogeneous. Based on the calculated values of the electric field strength at the edge of the rod electrode, the maximum Joule heat release occurs, reaching values of $11\,000\,\text{W/cm}^3$, later in this region the process of vapor-gas mixture formation occurs with further breakdown (Fig. 5, b). In the direction of the electrolyte the power density of the Joule heat release rapidly decreases, which is due to decrease in the electric field strength.

Let us estimate the characteristic time of vaporization τ due to Joule heat release (4). If we neglect the processes of heat capacity and thermal conductivity, all the released power is used for vaporization:

$$\sigma E^2 \Delta V \tau = r\rho\Delta V.$$

Here r — specific heat of vaporization, ρ — density of water, ΔV — small volume of electrolyte. It follows that

$$\tau = \frac{r\rho}{\sigma E^2}.$$

From Fig. 5, b the maximum value of $w = \sigma E^2$ near the electrode is equal to $\sim 1.1 \cdot 10^4\,\text{W/cm}^3$. Substituting this value, we get $\tau \approx 0.02\,\text{s}$.

The properties of gas-discharge plasma are measured, as a rule, using probe methods, however, in HF discharges with liquid (non-metallic) electrodes the probe diagnostics is difficult due to the high dynamics of the processes occurring in the discharge burning zone, electrolyte boiling and splashing, small plasma volumes, the influence of magnetic field, and probe destruction. The spectroscopic method of diagnostics [21] was chosen to eliminate perturbation and contact with the plasma under study, as well as to ensure immunity to electromagnetic interference. At the same time, a shortcoming of the spectroscopic method is that the radiation is collected from the entire volume of the plasma, which makes it difficult to determine to which discharge region the parameters refer to.

In the studied spectrum of HF discharge (Fig. 6) the instrumental broadening was checked along the K I atomic line (766.45 nm). The minimum width of optically thin and

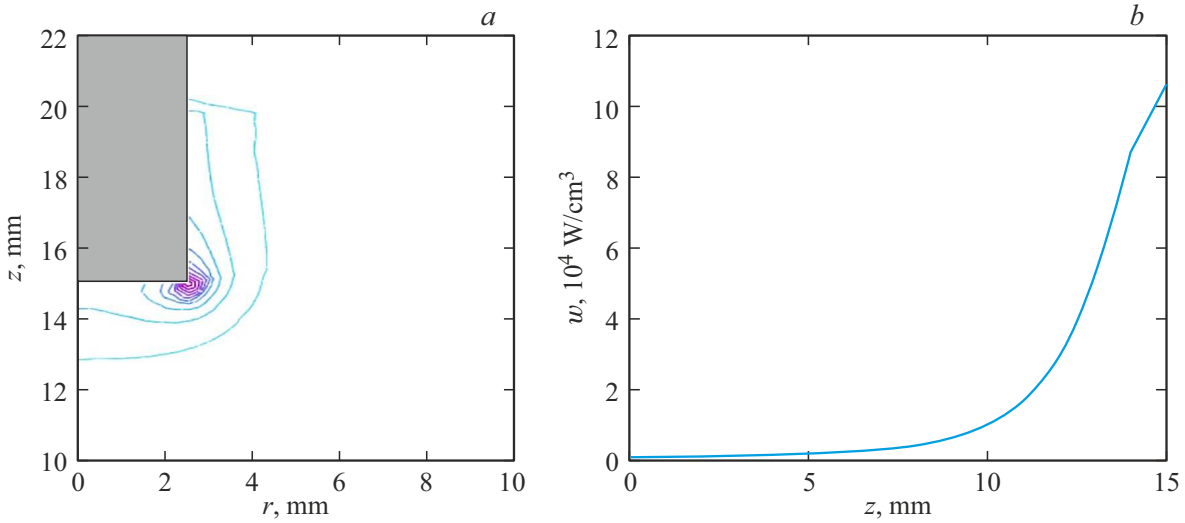

Figure 5. Distribution of the volumetric power density of the Joule heat release (a) and the volumetric power density of the Joule heat release w on the symmetry axis ($r = 0$) in the gap from the bottom plate to the electrode (it b).

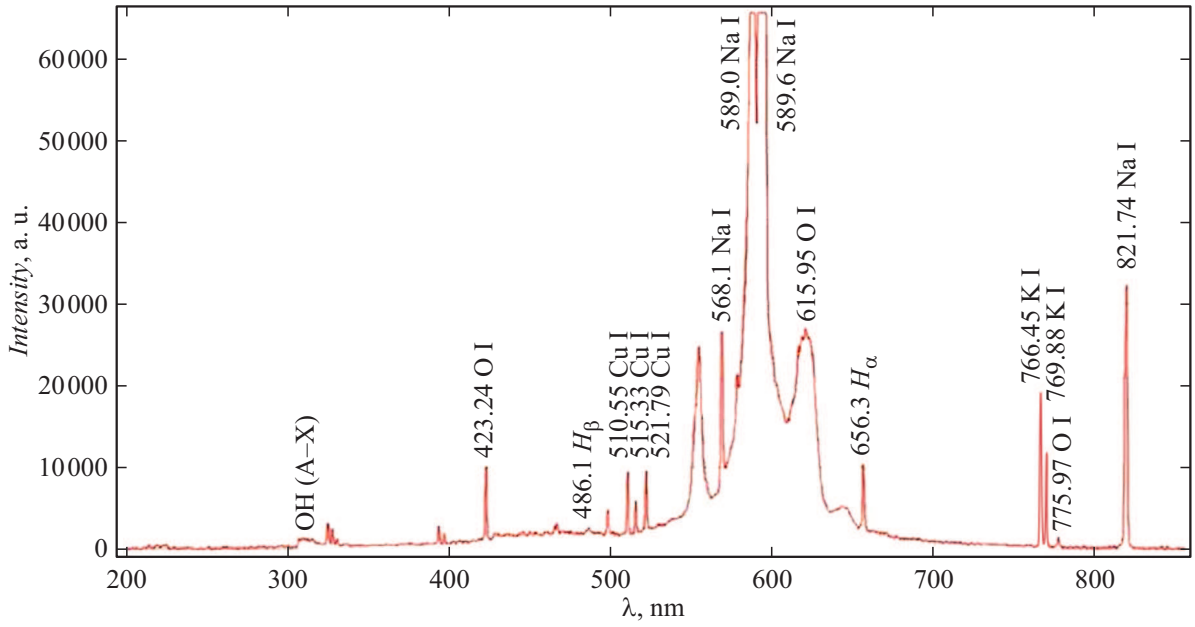

Figure 6. Spectrum under study with identified spectral lines.

narrowest lines was $\Delta\lambda G \approx 1$ nm, — and it was taken as the instrumental width. The emitting components of the spectra are presented in Table 1. An estimate of the electron density in the HF discharge plasma was calculated from the half-width of several hydrogen lines from the Balmer series (Table 2). The half-width of the Voigt contour $\Delta\lambda_F$ of H_α line turned out to be 1.45 nm.

Taking into account the instrumental component, the line broadening due to pressure effects (Lorentzian width) of the line was determined by the formula

$$\Delta\lambda_F \approx 0.5346\Delta\lambda_L + \sqrt{0.2166\Delta\lambda_L^2 + \Delta\lambda_G^2},$$

Table 1. Emitting components of the spectrum

Atoms	Hydrogen H I, Oxygen O I, Potassium K I, Copper Cu I, sodium Na I
Molecules	OH (A-X)
Continuum	300–700 nm

where $\Delta\lambda_G$ — Gaussian contour width, $\Delta\lambda_F$ — Voigt contour width, $\Delta\lambda_L$ — Lorentzian contour width. For the hydrogen line H_α from the Balmer series, the width of the Lorentzian contour is $\Delta\lambda_L = 0.74$ nm.

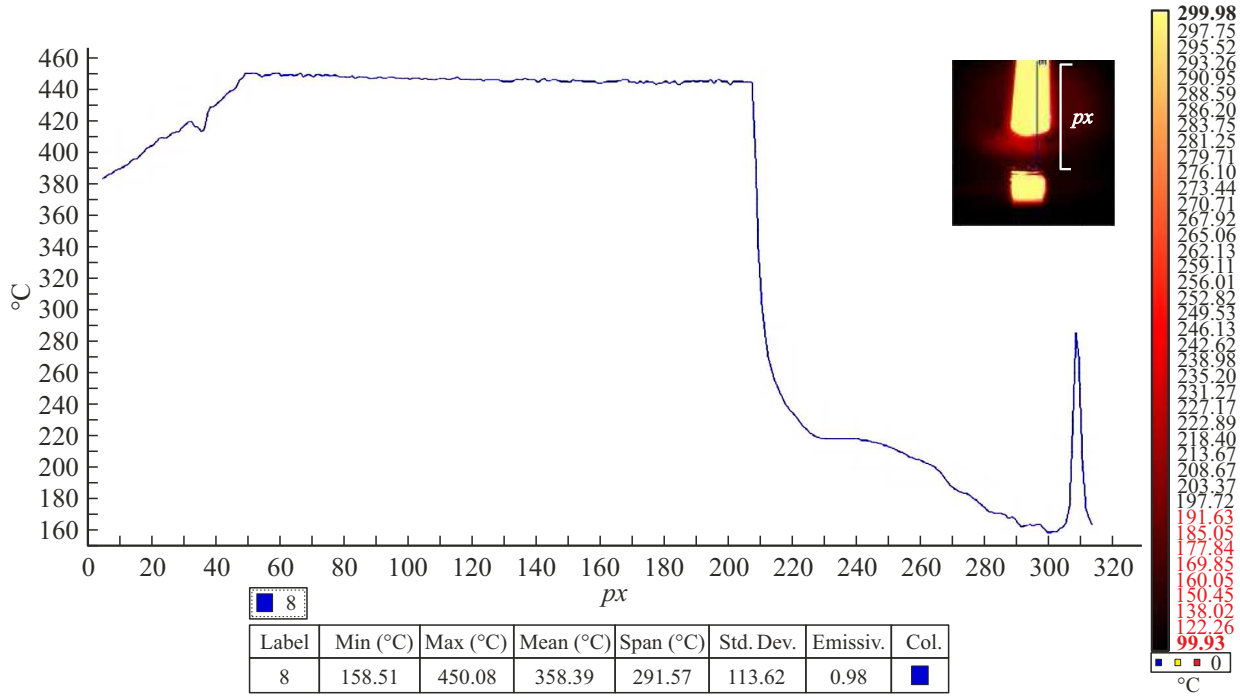

Label	Min (°C)	Max (°C)	Mean (°C)	Span (°C)	Std. Dev.	Emissiv.	Col.
8	158.51	450.08	358.39	291.57	113.62	0.98	

Figure 7. Thermogram of the surface of metallic and electrolytic electrodes under conditions of high-frequency discharge burning.

Table 2. Half-width and electron density by hydrogen lines from the Balmer series (H_α)

Parameters	$\Delta\lambda_f$, nm	$\Delta\lambda_L$, nm
Half-width by H_α, nm	1.45	0.74
Electron density, cm^{-3}	$1.8 \cdot 10^{16}$	$7.7 \cdot 10^{16}$

According to the reference book [22], for H_α the value $\Delta\lambda_L = 1.45$ nm corresponds to the concentration $n_e = 7.7 \cdot 10^{16}\,cm^{-3}$, and the electron density was checked using the graphic dependence in the paper [23], based on which the half-width H_α approximately corresponds to the concentration $n_e = 1.8 \cdot 10^{16}\,cm^{-3}$.

The thermograms of the surface of metallic and electrolytic electrodes were studied during the HF discharge combustion between them (Fig. 7). The temperature of the electrode surface was estimated in the vertical plane *px*. Based on the analysis of the obtained data, it follows that at distance from 0 to 50 mm the surface temperature of the metallic electrode rises from 380 to 450°C. Then the temperature stabilizes and does not change at distance from 50 to 205 mm. In the region of the interelectrode gap from 205 to 300 mm, the temperature decreases to 160°. At distance from 307 to 310 mm a sharp increase in temperature up to 290°C is observed, which corresponds to the spot zone on the electrolyte surface.

So, in paper the properties of HF discharge were studied when metallic electrode was immersed in the electrolyte at atmospheric pressure. To interpret the breakdown conditions in the gas-vapor mixture near metal electrode, the numerical calculations of the electric field strength and the distribution of the volumetric power density of the Joule heat release were carried out.

Conclusion

It was established that the HF discharge between the metallic and electrolytic electrodes is formed in the form of microchannels in the voltage range from 1 to 3 kV, which pulsate in the vapor-air mixture around the metallic electrode. With increase in voltage over 3.5 kV, the RF discharge passes into the volumetric (diffuse) combustion mode with discharge current fluctuations from 10 to 18 A.

The results of numerical calculations of the electric field strength and the distribution of the volumetric power density of the Joule heat release are presented. Near the metallic electrode the electric field strength reaches 210 V/mm. The greatest heat release occurs near the edge of the electrode, where the electric field is highly heterogeneous. Based on the calculated values of the electric field strength at the edge of the rod electrode, the maximum Joule heat release occurs, reaching values of 11 000 W/cm^3, later in this region the process of vapor-gas mixture formation occurs with further breakdown. The characteristic time of vaporization due to Joule heat release is $\tau \approx 0.02$ s.

Based on the analysis of the spectral parameters of the HF discharge, it can be seen that the discharge plasma contains lines of hydrogen H I, oxygen O I, potassium K I, copper Cu I, sodium Na I, and hydroxyl OH group. The

electron density estimated from the hydrogen lines of the Balmer series (H_α) turned out to be $n_e = 1.8 \cdot 10^{16}\,\mathrm{cm}^{-3}$.

It can be seen from the analysis of the thermograms that the temperature of the loaded metallic electrode increases from 380 to 450°C in the direction of the RF discharge. A temperature peak increase up to 290°C was found in the region of the plasma spot on the electrolyte surface.

Funding

This study was supported financially by the Russian Science Foundation (project №. 22-29-00021).

Conflict of interest

The authors declare that they have no conflict of interest.

References

[1] P.J. Bruggeman, A. Bogaerts, J.M. Pouvesle, E. Robert, E.J. Szili. J. Appl. Phys., **130** (20), 200401 (2021). DOI: 10.1063/5.0078076
[2] N.F. Kashapov, R.N. Kashapov, L.N. Kashapov. J. Phys. D: Appl. Phys., **51** (49), 494003 (2018). DOI: 10.1088/1361-6463/aae334
[3] D.T. Elg, H.E. Delgado, D.C. Martin, R.M. Sankaran, P. Rumbach, D.M. Bartels, D.B. Go. Spectrochimica Acta Part B: Atomic Spectroscopy, **186**, 106307 (2021). DOI: 10.1016/j.sab.2021.106307
[4] A.F. Gaisin, N.F. Kashapov, A.I. Kuputdinova, R.A. Mukhametov. Tech. Phys., **63** (5), 695 (2018). DOI: 10.1134/S1063784218050080
[5] A.V. Khlyustova. ZhTF, **47**, 38 (2021) (in Russian). DOI: 10.21883/PJTF.2021.19.51512.18882
[6] P. Andre, Y. Barinov, G. Faure, V. Kaplan, A. Lefort, S. Shkol'nik, D. Vacher. J. Phys. D: Appl. Phys., **34** (20), 3456 (2001). DOI: 10.1088/0022-3727/34/24/306
[7] V.A. Panov, L.M. Vasilyak, S.P. Vetchinin, V.Ya. Pecherkin, A.S. Saveliev. Plasma Phys. Reports, **44**, 882 (2018). DOI: 10.1134/S1063780X1809009X
[8] D.L. Kirko, Plasma Phys. Reports, **46**, 597 (2020). DOI: 10.1134/S1063780X20060045
[9] L.N. Bagautdinova, R.Sh. Sadriev, Az.F. Gaysin, S.Ch. Mastyukov, F.M. Gaysin, I.T. Fakhrutdinova, M.A. Leushka, Al.F. Gaysin. High Temperature, **57**, 944 (2019). DOI: 10.1134/S0018151X19060051
[10] E.I. Meletis, X. Nie, F.L. Wang, J.C. Jiang. Surf. Coat. Technol., **150**, 246 (2002). DOI: 10.1016/S0257-8972(01)01521-3
[11] T. Ishijima, K. Nosaka, Y. Tanaka, Y. Uesugi1, Y. Goto, H. Horibe. Appl. Phys. Lett., **103**, 142101 (2013). DOI: 10.1063/1.4823530
[12] Al.F. Gaysin. Inorganic Mater.: Appl. Research, **8**, 392 (2017). DOI: 10.1134/S207511331703008X
[13] A.F. Gaysin, A.K. Gil'mutdinov, D.N. Mirkhanov. Metal. Sci. Heat Treatment, **60**, 128 (2018). DOI: 10.1007/s11041-018-0250-1
[14] E.E. Son, I.F. Suvorov, S.V. Kakurov, Al.F. Gaisin, G.T. Samitova, T.L. Solov'eva, A.S. Yudin, T.V. Rakhletsova. High Temperature, **52**, 490 (2014). DOI: 10.1134/S0018151X14040208
[15] Y.P. Raizer, M.N. Shneider, N.A. Yatsenko. *Radio-Frequency Capacitive Discharges* (CRC Press, London, 1995), p. 304. DOI: 10.1201/9780203741337
[16] Y. Sakiyama, D.B. Graves, Chang Hung-Wen, T. Shimizu, G.E. Morfill. J. Phys. D: Appl. Phys., **45**, 425201 (2012). DOI: 10.1088/0022-3727/45/42/425201
[17] Y.P. Raizer, J.E. Allen, V.I. Kisin. *Gas Discharge Physics* (Springer, Berlin, 1997), p. 449.
[18] A.F. Gaisin, F.M. Gaisin, V.S. Zheltukhin, E.E. Son. Plasma Phys. Reports, **48**, 48 (2022). DOI: 10.1134/S1063780X22010068
[19] V.S. Zheltukhin, Al.F. Gaisin, S.Yu. Petryakov. Pis'ma v ZhTF **48**, 24 (2022) (in Russian). DOI: 10.21883/PJTF.2022.17.53283.19237
[20] I.N. Sadovsky, A.V. Kuzmin, E.A. Sharkov, D.S. Sazonov, E.V. Pashinov, A.A. Asheko, S.A. Batulin. *Analiz modelej dielektricheskoj pronitsaemosti vodnoj sredy ispol'zuemykh v zadachakh distantsionnogo zondirovaniya akvatorij* (IKI RAN, M., 2013), s. 59. (in Russian)
[21] V.V. Antsiferov. ZhTF, **68** (10), 32 (1997) (in Russian).
[22] G.A. Kasabov, V.V. Eliseev. *Spektroskopicheskie tablitsy dlya nizkotemperaturnoj plazmy: spravochnik*(Atomizdat, M., 1973), s. 160. (in Russian)
[23] V.N. Ochkin, *Spektroskopiya nizkotemperaturnoi plazmy* (Fizmatlit, M., 2006), s. 472 (in Russian).

Translated by I.Mazurov